05

Study of the influence of pressure and electric field on the material emission and deposition rate of Al_2O_3 and ZrO_2 in the process of pulsed laser deposition

© M.I. Vasilyev, Yu.D. Dudnik, A.A. Safronov, V.N. Shiryaev, O.B. Vasilieva

Institute for Electrophysics and Electric Power, Russian Academy of Sciences, St. Petersburg, Russia

e-mail: milavas@mail.ru, julia_dudnik-s@mail.ru

Received February 20, 2025
Revised February 20, 2025
Accepted July 12, 2025

The deposition of coatings on steel substrates from thin alternating layers consisting of aluminum oxide and yttrium-stabilized zirconium oxide in a vacuum chamber in an oxygen atmosphere was studied using pulsed laser deposition using a KrF excimer laser with an emission wavelength of 248 nm. To increase the deposition rate of ablated particles, an electric field was applied between the substrate and the target during the processing. The effect of an electric field of different polarity on the deposition rate was studied at different oxygen pressures in the vacuum chamber. The spectral intensity of the plasma plume of atoms and ionized particles was measured during the processing in order to study the particle composition in the plasma plume. The evolution of plasma plume images at different oxygen pressures in the vacuum chamber was recorded and processed.

Keywords: pulsed laser deposition, laser ablation, thin films, plasma plume, emission spectra.

DOI: 10.61011/EOS.2025.09.62305.7627-25

Introduction

Thin-film coatings attract significant interest in the optical, electronic, and aerospace research communities. The scientific literature describes numerous methods for fabricating such coatings. Pulsed laser deposition (PLD) [1–6], using laser ablation techniques, has been recognized as one of the most technologically versatile and cost-effective methods for growing thin films. In this technique, a focused pulsed laser beam with high power density is used to ablate coating materials from a metallic or ceramic target. The laser pulse interaction with the target generates a plasma plume, whose products deposit onto the substrate surface. The PLD method can also be applied to create coatings from materials that are difficult to deposit by other means.

The laser-induced plasma, moving toward the substrate, consists of atoms, partially ionized target atoms, electrons, and ionized gases within the vacuum chamber. The movement of charged particles in the plasma can be influenced by external electric and magnetic fields. Previous attempts to achieve desired material properties and improve coating quality have involved auxiliary methods integrated into the traditional PLD process. Essentially, these methods applied a direct current (DC) electric field to the plasma plume composed of negatively or positively charged particles, thereby affecting their motion during PLD.

Lubben et al. [7] applied a constant voltage bias by imposing an electric field between the target and substrate during PLD to deposit semiconductor epitaxial films of germanium and silicon. Applying a negative bias significantly reduced the particle density embedded in the resulting film. The particle density for the sample deposited on the substrate at a bias voltage up to -150 V was about five times lower than without bias.

In the study [8], a DC bias voltage was used in PLD to deposit superconducting films of Y–Ba–Cu–O. A high-voltage ring electrode was placed between the substrate and target to promote the formation of O_2^+ ions by ionizing O_2molecules supplied in an oxygen flow. This led to increased oxygen content in the deposited film and enhanced its superconducting properties.

A similar technique for improving superconducting film properties was employed in [9]. However, the exact effect of the ring voltage application, as well as its polarity, on deposition quality could not be conclusively determined. Later, in [10], the use of bias voltage during PLD for superconducting thin film deposition was also reported. The substrate bias voltage improved not only the electrical properties but also the surface morphology. According to these results, a positive bias was more effective than a negative one.

Experiment

In this study, an external electric field of varying strength and polarity was applied to influence the charged products of the laser plasma and consequently increase the amount of material collected on the substrate. Images and emission spectra of the plasma plume were analyzed to gain a comprehensive understanding of the film growth conditions. The PLD experiment was conducted in a stainless steel vacuum chamber using oxygen as the reactive gas. Half of the target consisted of hot-pressed zirconium dioxide (ZrO2) stabilized with 5% mass $Y_2O_3$and the other half

was aluminum oxide Al_2O_3; both materials were used to deposit thin alternating layers on steel substrates. A KrF excimer laser with a wavelength of 248 nm was used to ablate the target material at a repetition rate of 10 Hz and pulse duration of ~ 20 ns. The pulse energy density ranged from 1.4 to 2.5 J/cm^2. The laser beam was focused to a 3 mm^2 area on the target at an incidence angle of $\sim 40°$. The distance between the ablation spot and the substrate center was ~ 25 mm.

To apply the electric field between the target and substrate, an additional ring-shaped metal electrode was placed directly above the target. The electrode was connected to a DC power supply. Two copper wires from the electrical feedthrough on the vacuum chamber's upper flange were connected to the metal substrate holder and the ring electrode above the target. The DC voltage was controlled by the power supply.

The deposition rate (mg/pulse) was determined by measuring the weight of material collected on the substrate using highly sensitive automatic scales AD-6 Perkin Elmer with a sensitivity of 0.1 microgram. Spectral intensity measurement of plasma plume emission was performed with a fast high-resolution spectrometer (HR 2000+, Ocean Optics Inc.) in the wavelength range of 268 to 486 nm with a spectral resolution of 0.08 nm. An LC-22 collimator from Multimode Fiber Optics, Inc., having no defined focal length (infinite focal length), was used. It allowed easy light collection from the plasma plume and direct connection via an SMA fiber optic interface to the spectrophotometer.

Images of the plasma plume at various oxygen gas pressures during ablation were obtained using a Nikon D80 digital camera with 10 megapixels and a maximum shutter speed of 1/4000 s.

Results and discussion

Effect of Electric Field on Deposition Rate

The relationship between the deposition rate, representing the amount of material collected on the substrate per pulse, and experimental variables was investigated. To study the effect of the electric field on the laser-induced plasma, the magnitude and polarity of the DC voltage, laser energy flux, and oxygen pressure in the chamber were varied.

Figure 1 shows the measured deposition rate [mg/pulse] at oxygen pressures in the vacuum chamber ranging from 10^{-5} to 5 Torr. The pulsed beam energy flux was about ~ 1.4 J/cm^{2}the pulse repetition rate was 10 Hz, and the processing time was 30 minutes, amounting to 18,000 pulses.

The deposition rate showed little change around the vacuum region $5 \cdot 10^{-5}$–$5 \cdot 10^{-4}$ Torr. At a pressure of $5 \cdot 10^{-5}$ Torr applying a negative voltage of -1 kV to the substrate increased the deposition rate by $\sim 15\%$ relative to zero applied voltage. At $5 \cdot 10^{-4}$ Torr the deposition rate slightly increased (by $\sim 10\%$) for -1 kV and zero voltage, whereas it decreased by approximately the same amount for

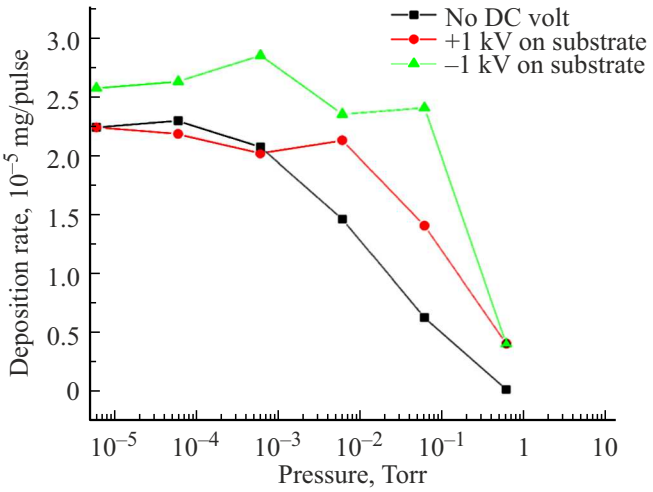

Figure 1. Dependence of deposition rate on gaseous oxygen pressure (pulse energy density ~ 1.4 J/cm^2).

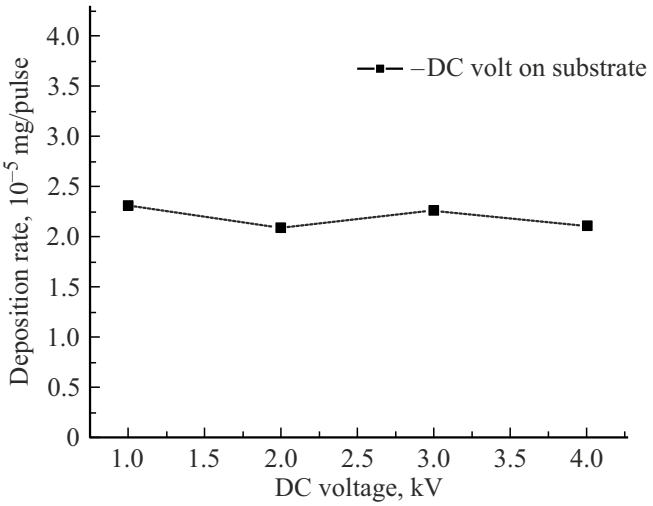

Figure 2. Dependence of deposition rate on applied negative voltage (vacuum $5 \cdot 10^{-4}$ Torr, pulse energy density ~ 1.4 J/cm^2).

positive $+1$ kV. From this, it can be inferred that the plasma plume is sufficiently strong and fast to deposit particles on the substrate even at relatively high vacuum.

Applying an electric field in the range from -1 to -4 kV (Figure 2) did not significantly affect the deposition rate enhancement. Obviously, the deposition rate is proportional to the laser beam energy flux at both high and low vacuum. Meanwhile, the electric field seemingly does not strongly influence the deposition rate in the relatively high vacuum region, as further seen in Figure 2.

As the gaseous oxygen pressure inside the chamber increased under electric fields of different polarity, the difference in deposition rates grew, despite an overall trend of decreasing deposition rate regardless of the presence of the electric field. For instance, at an oxygen pressure of 0.5 Torr, when -10^3 V was applied to the substrate, the collection rate increased to $\sim 290\%$ relative to deposition

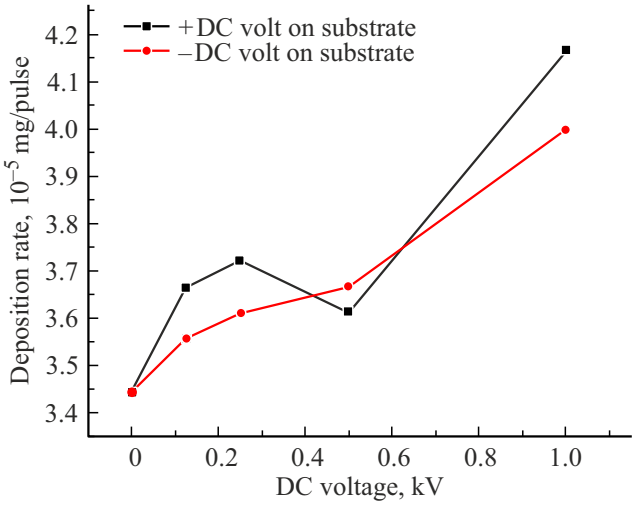

Figure 3. Dependence of deposition rate on applied voltage (oxygen gas pressure 0.1 Torr, pulse energy density $\sim 2.5\,\mathrm{J/cm^2}$).

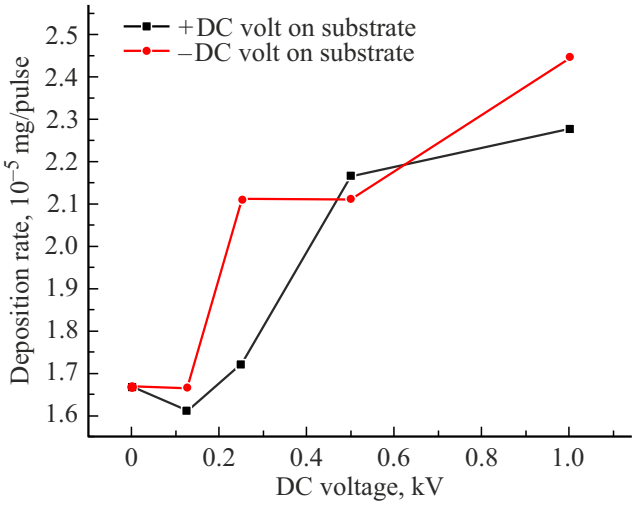

Figure 4. Dependence of deposition rate on applied voltage (oxygen pressure 0.1 Torr; pulse energy density $\sim 1.8\,\mathrm{J/cm^2}$).

at the same pressure without applied voltage. This can be explained by the different effects of the field on the motion of charged particles in the expanding plasma plume at that gas pressure.

However, as shown in Figures 3 and 4, when the chamber was filled with gaseous oxygen at a pressure of 0.1 Torr and at a pulse energy flux of $\sim 2.5\,\mathrm{J/cm^2}$ (Fig. 2, *a*), the collection rate gradually increased by $\sim 20-25\%$ with increasing DC voltage from 0 to ± 1 kV. Moreover, at the lower energy flux ($\sim 1.8\,\mathrm{J/cm^2}$) (Figure 4), a similar trend of increasing deposition rate with rising applied voltage was observed. When a DC voltage of -1 kV is applied to the substrate, the collection rate increases by 47% at a lower pulse energy flux ($\sim 1.8\,\mathrm{J/cm^2}$). This indicates that applying an electric field effectively enhances the collection rate both when the plasma plume is generated by a pulsed beam with

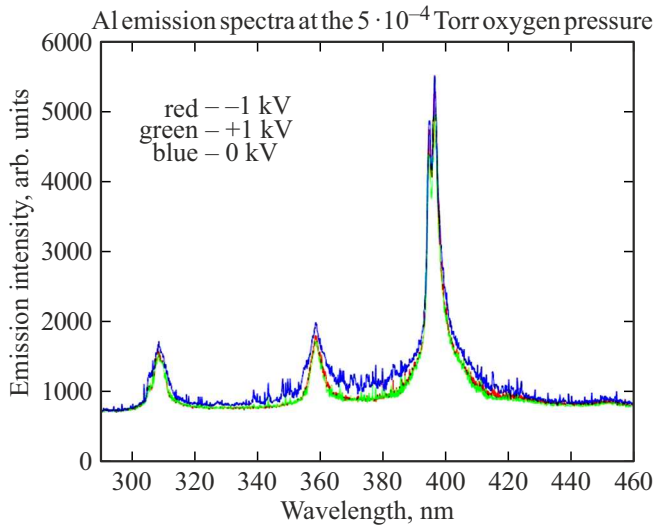

Figure 5. Al emission intensity spectrum at an oxygen pressure of $5 \cdot 10^{-4}$ Torr.

low energy density and when generated at a higher energy density (Fig. 3).

From a series of experiments, it can be concluded that an electric field can be used to increase the deposition rate when there are some restrictions on the expansion of the plasma plume due to collisions with the ambient gas or when a weak plasma jet is generated by a laser pulse with low energy.

Emission Spectroscopy Results

Spectra of the pulsed laser deposition emission of the target material, consisting of two parts — hot-pressed ZrO_2 stabilized with 5% mass Y_2O_3) and Al_2O_3 — were recorded. The operating wavelength of the KrF excimer laser used was 248 nm, which is far from the spectral range of −486 nm HR2000+ Ocean Optics spectrometer used in the experiment. To collect sufficient light, an integration time of 500 ms was used. The laser repetition rate was 10 Hz, so during one spectral acquisition, five pulses were recorded. The following strong emission lines of aluminum and zirconium atoms and ions were present in the selected spectral range:

Al I 309.27 nm $3s^23p-3s^23d$, 394.40 nm $3s^23p-3s^24s$, 396.15 nm $3s^23p-3s^24s$;

Al II 358.74 nm $3s3d-3s4f$;

Zr I 383.68, 423.93, 450.51, 457.55, 460.26, 462.64, 468.78, 471.01, 473.95, 477.23, 478.87, 48.56 nm;

Zr II 404.86, 414.92, 420.90, 444.30, 449.70 nm.

It should be noted that the emission spectra of Zr I and II contain about 355 lines in the indicated spectral range according to NIST data [11]. In our measured emission spectra, well-resolved lines mentioned above were observed. To determine the influence of the electric field on the deposition rate on the substrate, zirconium plasma emission intensity spectra were measured with electric fields

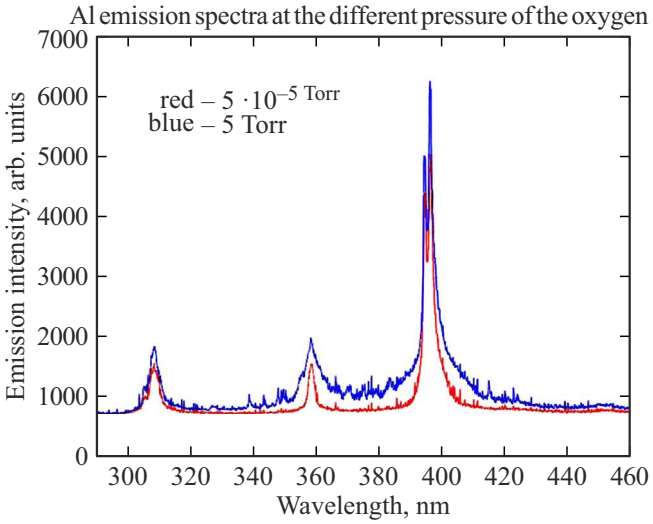

Figure 6. Al emission intensity spectrum at different oxygen pressures (without applied electric field).

of +1, −1 kV and without the field applied at an oxygen pressure of $5 \cdot 10^{-4}$ Torr. Notably, no significant increase in deposition rate was observed at relatively high vacuum. No substantial effect of the applied electric field on zirconium emission spectra was detected. It is difficult to comment on the broadening of Zr emission lines without additional experiments.

In the Al_2O_3 emission spectra at pressures ranging from $5 \cdot 10^{-5}$ to 5 Torr strong Al I 309.27 ($3s^2 3p - 3s^2 3d$), Al II within 358 nm ($3s3d - 3s4f$), Al I 394.40 and 396.15 nm lines were observed.. At an oxygen pressure of $5 \cdot 10^{-4}$ Torr the applied electric field of both+1, and −1 kV resulted in reduced broadening of Al emission spectral lines compared to zero field (Fig. 5).

This broadening may be explained by strong interactions with the surrounding oxygen atmosphere in the chamber as pressure increases. The obvious effect of pressure on emission spectra can be observed in Fig. 6. The wings of the Al I 394.40 nm and 396.15 nm lines are elevated, and broadening of the Al II 358.74 nm line $3s3d - 3s4f$ is observed at lower vacuum. This clearly indicates interaction between emitting or absorbing particles and surrounding oxygen. For example, Lorentzian fitting of the Al I 394.40 nm line at 5 Torr yields a full width at half maximum (FWHM) of about 90 $cm^{-1}$and about 120 cm for 396.15 nm $^{-1}$. The observed increase in Al emission line widths with increasing oxygen pressure is attributed to intensified heating and ionizing effects of shock waves formed at the boundary between the expanding erosion material from the target and the gas atmosphere.

Digital Imaging of the Plasma Plume

Figure 7 shows images of the plasma jet during the ablation process captured by a Nikon D80 digital camera at various oxygen gas pressures. The experiment consisted of three series. For all series, the pulse energy was the same at ~ 1.4 J/cm^2. In the first series (left column), the target was aluminum oxide Al^2O_3. In the second series (middle column), the target was hot-pressed zirconium dioxide ZrO_2 stabilized with 5% mass yttrium oxide Y_2O_3. In the third series (right column), half of the target was ZrO_2 and the other half was Al_2O_3. It can be noted that at sufficiently high vacuum $5 \cdot 10^{-5} - 5 \cdot 10^{-4}$ Torr, the plasma jet freely propagates directly to the substrate for both aluminum oxide and zirconium oxide. The same propagation behavior applies to the mixed target series. Different plasma zones emanating from Al_2O_3 and ZrO_2 are visible in the right column images. As the pressure rises — that is, as the number of oxygen molecules in the chamber increases — the moving plasma front collides with surrounding oxygen molecules, inhibiting free motion and causing plume expansion and a change in image coloration due to shock ionization. This is evident in the figure: starting at 0.05 Torr pressure, plume broadening and intense blue glow appear in the aluminum target plume, reaching the substrate. The plasma jet enlarges and its boundaries become blurred. In the middle column of Fig. 7, at an oxygen pressure of 0.5 Torr, the plasma emission exhibits sharp outlines. The plasma plume is constricted and its boundaries are clearly defined for both Zr and Al, indicating enhanced interaction between the plume and oxygen. With further pressure increases, the plume narrows, eventually failing to reach the substrate at around 0.5 Torr or above. This implies that when the plasma expansion is insufficiently strong, the electric field may influence the attraction of plasma ions toward the substrate, as seen in Fig. 1. This leads to some increase in the deposition rate relative to the case without applied electric field at the same pressure, although the overall trend of decreasing deposition rate with increasing oxygen pressure holds.

At pressures of 0.5 and 5 Torr, in all three cases the plasma plume is sharply defined, pressed against the target, and does not contact the substrate, suggesting a significant decrease in deposition rate. This is consistent with the results shown in Fig. 1.

The Nikon D80 camera used employs a Bayer filter — a two-dimensional array of three spatially separated color filters covering the photodiodes of the sensor. The color image is formed by the Bayer filter consisting of 25% red, 25% blue, and 50% green photofilters with corresponding spectral transmission bands. We processed the plasma jet images by separately analyzing the two-dimensional matrices of blue (B), green (G), and red (R) colors. Figure 8 presents plasma plume images from the aluminum target at oxygen pressures of $5 \cdot 10^{-5}$, $5 \cdot 10^{-3}$ and $5 \cdot 10^{-2}$ Torr, and from the zirconium target at $5 \cdot 10^{-3}$ Torr oxygen pressure.

It can be noted that with increasing oxygen pressure, the plasma plume gradually expands in the images obtained with red and green filters. At $5 \cdot 10^{-2}$ Torr oxygen pressure, the aluminum plasma jet reaches the substrate. At $5 \cdot 10^{-3}$ Torr during zirconium target ablation, the plasma plume contacts the substrate. The plume notably expands in

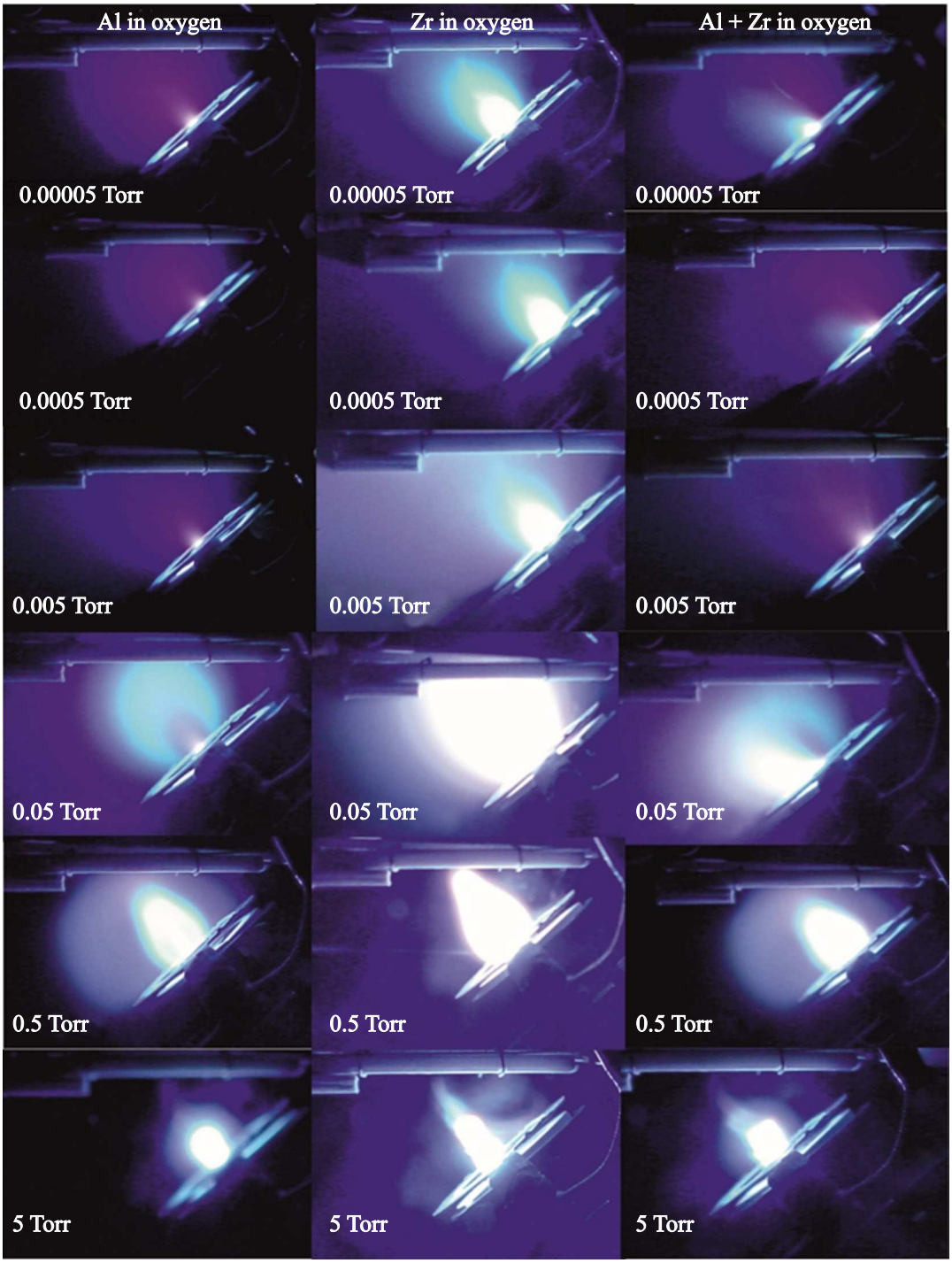

Figure 7. Plasma plume images at different oxygen pressures: Al, Zr, mixture of Al:Zr in ratio 1 : 1.

blue-filtered images, showing intense ionizing effects of the shock wave formed at the interface between the expanding target erosion material and the oxygen atmosphere. This correlates well with emission spectra in the blue spectral range for both zirconium dioxide $ZrO_2$and aluminum oxide Al_2O_3. As seen in the figure, plasma plume expansion is observed at pressures of 0.05 Torr and above, with especially marked expansion in the blue (B) filtered images, correlating well with emission spectra of zirconium dioxide $ZrO_2$and aluminum oxide Al_2O_3.

Conclusion

The effect of an electric field on the deposition rate during PLD was investigated. The electric field created between

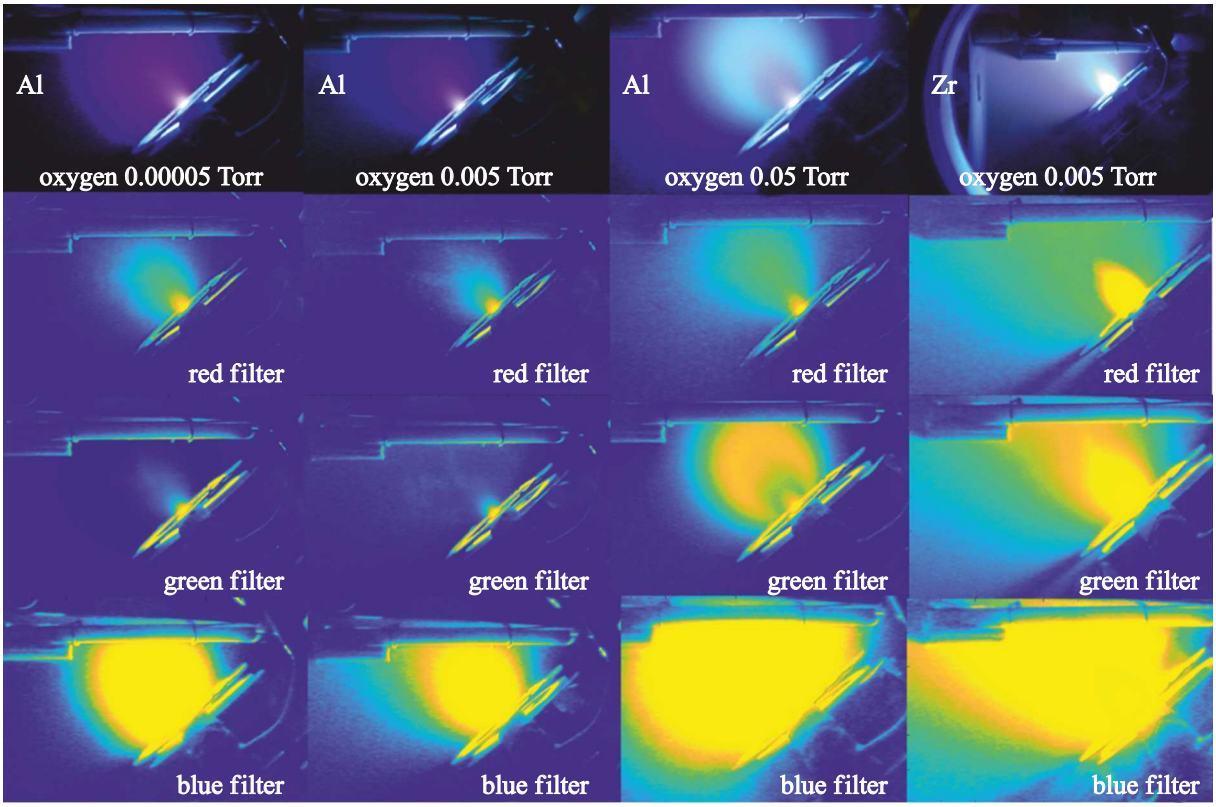

Figure 8. Plasma plume images processed with red, green, and blue filters.

the target and substrate by applying bias voltages was found to be quite effective in increasing the deposition rate when the buffer gas pressure was $5 \cdot 10^{-5}-5 \cdot 10^{-4}$ Torr. At 0.1 Torr pressure, using an electric field at a pulsed energy of $\sim 1.8\,\mathrm{J/cm^2}$ was more effective compared to the higher energy pulse of $\sim 2.5\,\mathrm{J/cm^2}$. At elevated pressures, the plasma jet cannot expand freely due to collisions with surrounding oxygen molecules, and when a weak plasma plume from a low-energy pulse is generated, the electric field can act as a driving force accelerating ionic species toward the substrate. Emission spectroscopy results revealed complex broadening of Al I spectral lines. Further studies are needed to clarify the interaction between the electric field and laser-induced plasma.

Conflict of interest

The authors declare that they have no conflict of interest.

References

[1] R. Aguiar, V. Trtik, F. Sanchez, C. Ferrater, M. Varela. Thin Solid Films, **304** (1–2), 225–228 (1997). DOI: 10.1016/S0040-6090(97)00201-0

[2] F. Sanchez, R. Aguiar, P. Serra, M. Varela, J.L. Morenza. Thin Solid Films, **317** (1–2), 108–111 (1998). DOI: 10.1016/S0040-6090(97)00604-4

[3] C.H. Lei, G. Van, Tendeloo, M. Siegert, J. Schubert, Ch. Buchal. J. Crystal Growth, **222**, 558–564 (2001). DOI: 10.1016/S0022-0248(00)00943-X

[4] Peng Li, Jason Carroll and Jyoti Mazumder. J. Phys. D, **36**, 1605–1608 (2003). DOI: 10.1088/0022-3727/36/13/327

[5] A.P. Caricato, A. Di Cristoforo, M. Fernandez, G. Leggieri, A. Luches, G. Majni, M. Martino, P. Mengucci. Appl. Surf. Sci., 208–209, 615–619 (2003). DOI: 10.1016/S0169-4332(02)01404-6

[6] A.P. Caricato, G. Barucca, A. Di Cristoforo, G. Leggieri, A. Luches, G. Majni, M. Martino, P. Mengucci. Appl. Surf. Sci., **248** (1–4), 270–275 (2005). DOI: 10.1016/j.apsusc.2005.03.048

[7] D. Lubben, S.A. Barnett, K. Suzuki, S. Gorbatkin, J.E. Greene. J. Vac. Sci. Technol. B, **3** (4), 968–974 (1985). DOI: 10.1116/1.583024

[8] S. Witanachchi, H.S. Kwork, X.W. Wang, D.T. Shaw. Appl. Phys. Lett., **53** (3), 234–236 (1988). DOI: 10.1063/1.100585

[9] R.K. Singh, L. Ganapathi, P. Tiwari, J. Narayan. Appl. Phys. Lett., **55** (22), 2351–2353 (1989). DOI: 10.1063/1.102364

[10] H. Izumi, K. Ohata, T. Hase, K. Suzuki, T. Morishita, S. Tanaka. J. Appl. Phys., **68** (12), 6331–6335 (1990). DOI: 10.1063/1.346877

[11] A. Kramida, Yu. Ralchenko, J. Reader, and NIST ASD Team. NIST Atomic Spectra Database (ver. 5.3). Electronic resource. Access mode: http://physics.nist.gov/asd.

Translated by J.Savelyeva